T-Square Dependence of the Electronic Thermal Resistivity of Metallic Strontium Titanate

Shan Jiang,[1] Benoît Fauqué,[2] and Kamran Behnia[1]
[1]Laboratoire de Physique et d'Étude des Matériaux (ESPCI Paris - CNRS - Sorbonne Université), PSL University, 75005 Paris, France
[2]JEIP, USR 3573 CNRS, Collège de France, PSL University, 75231 Paris Cedex 05, France

(Received 12 April 2023; accepted 13 June 2023; published 6 July 2023)

The temperature dependence of the phase space for electron-electron (e-e) collisions leads to a T-square contribution to electrical resistivity of metals. Umklapp scattering is identified as the origin of momentum loss due to e-e scattering in dense metals. However, in dilute metals like lightly doped strontium titanate, the origin of T-square electrical resistivity in the absence of umklapp events is yet to be pinned down. Here, by separating electron and phonon contributions to heat transport, we extract the electronic thermal resistivity in niobium-doped strontium titanate and show that it also displays a T-square temperature dependence. Its amplitude correlates with the T-square electrical resistivity. The Wiedemann-Franz law strictly holds in the zero-temperature limit, but not at finite temperature, because the two T-square prefactors are different by a factor of ≈3, like in other Fermi liquids. Recalling the case of ^{3}He, we argue that T-square thermal resistivity does not require umklapp events. The approximate recovery of the Wiedemann-Franz law in the presence of disorder would account for a T-square electrical resistivity without umklapp.

DOI: 10.1103/PhysRevLett.131.016301

Landau and Pomeranchuk [1], and contemporaneously Baber [2], postulated that electron-electron collisions cause a quadratic temperature dependence in electrical resistivity of metals. Subsequent experiments found that this is prominent in metals hosting strongly correlated electrons [such as UPt_3 [3] or strontium titanate (STO) [4]], and also those with a small carrier concentration (like bismuth [5] and graphite [6]). In these cases, at sufficiently low temperature, resistivity ρ can be expressed as $\rho = \rho_0 + AT^2$. ρ_0 depends on disorder, but A is intrinsic to each metal. Its ubiquitous relevance across families of Fermi liquids raises two questions. (1) What makes the exchange of momentum between two colliding electrons detrimental to the electrical conduction? (2) What sets the amplitude of A?

Two identified answers to the first question are umklapp and the Baber mechanism. An umklapp event occurs when the momentum vector sum of the colliding electrons gets out of the Brillouin zone, leading to a loss of momentum equivalent to one reciprocal unit vector [7,8]. The Baber mechanism [2] refers to the existence of two distinct electron reservoirs whose momentum exchange is a bottleneck in the path of momentum leak from the electron bath to the phonon bath. The second question was addressed first by Rice [9] and then by Kadowaki and Woods [10] (see also Refs. [11,12]), who argued that A scales with the square of the T-linear specific heat γ^2 because both depend on the density of states.

The persistence of T-square electric resistivity in metallic strontium titanate [13,14] to the extreme dilute limit [15] raised new questions about both answers. The Fermi surface in this dilute metal is too small to allow umklapp scattering and consists of a single pocket in the extreme dilute limit [16–18]. Thus, none of the two mechanisms can generate T-square resistivity. Moreover, the proper scaling relation was found to be between A and the Fermi energy, $A \propto E_F^{-2}$, instead of the standard Kadowaki-Woods scaling, $A \propto \gamma^2$, which fails in STO [19].

Following this observation, transport properties of dilute metallic STO were studied up to temperatures well above room temperature [20] and the effective mass was found to increase with warming. Two theoretical studies [21,22] showed that the temperature dependence of electrical resistivity in STO can be explained with a scenario based on the scattering of electrons by two soft transverse optical (TO) phonons. This would account for the persistence of T-square resistivity above the degeneracy temperature. On the other hand, low-temperature T-square resistivity (well below the minimum energy of TO phonons) remained a mystery. Another development was the discovery of T-square resistivity in dilute metallic Bi_2O_2Se [23], another solid with a small Fermi surface, and without any soft phonon mode. The T-square prefactor was found to scale with the Fermi energy. This demonstrated that STO is not an isolated case and called for an e-e scattering scenario in the absence of umklapp.

The T-square *thermal* resistivity of electrons in Fermi liquids is less known and even much less explored.

Defining the electronic thermal resistivity as $WT = T/\kappa^e$, one expects

$$WT = (WT)_0 + BT^2. \quad (1)$$

Here, $(WT)_0$ is the residual thermal resistivity, expected to obey the Wiedemann-Franz (WF) law: $L_0(WT)_0 = \rho_0$ with $L_0 = (\pi^2/3)(k_B^2/e^2) = 2.44 \times 10^{-8}$ V^2 K^{-2}. On the other hand, $L_0 B > A$, because, compared to energy flow, momentum flow is less affected by small-angle scattering [24,25]. Experiments on various metals, including Ni [26], Al [27], W [28], Sb [29], $CeRhIn_5$ [30], WP_2 [31], and UPt_3 [32], have confirmed both these expectations.

A quantitative connection between this physics and normal liquid ^{3}He was recently highlighted [33]. In ^{3}He, thermal conductivity becomes proportional to the inverse of temperature [34] at very low temperatures. Thus, thermal resistivity ($WT = T/\kappa$) is proportional to T^2. The evolution of this T-square resistivity with pressure follows the scaling seen for A and B with E_F in metals [33]. There is no umklapp in normal liquid ^{3}He and the Fermi surface is a single sphere. Thus, T-square thermal resistivity can occur in a Fermi liquid without umklapp and the amplitude of B is directly linked to its Landau parameters, which set the Fermi temperature.

Here, we present a study of electric and thermal conductivity in $SrTi_{1-x}Nb_xO_3$ at two different carrier concentrations ($n = 3.1 \times 10^{20}$ cm^{-3} and $n = 1.8 \times 10^{20}$ cm^{-3}). Despite the dominance of the lattice contribution [35–37], we succeeded in extracting the electronic contribution by exploiting the differentiating effect of the magnetic field on phonons and electrons, a method previously employed in the case of semimetals [29,38–40]. We found that WT follows Eq. (1) and $L_0 B > A$. Thus, T-square resistivity in $SrTi_{1-x}Nb_xO_3$ is similar to metals in which the e-e origin of the T-square resistivity is uncontested. This leads us to conclude that T-square (electric and thermal) resistivity can be caused without umklapp as a consequence of the T-square decrease in the amplitude of the (momentum and energy) diffusivity in a Fermi liquid. A comprehensive theory of this phenomenon is yet to be elaborated.

Figure 1 shows the temperature dependence of thermal conductivity in two samples of $SrTi_{1-x}Nb_xO_3$. The relatively low value residual resistivity of our samples is discussed in the Supplemental Material [41]. In order to see the relative share of the electronic and the phononic contributions to the total heat transport, κ_{xx}/T is compared with $L_0\sigma_{xx}$, which represents the upper boundary of electronic thermal conductivity according to the WF law. With decreasing temperature, κ_{xx}/T approaches $L_0\sigma_{xx}$. As the temperature tends to zero (see inset), they tend to join each other. κ_{xx}/T and $L_0\sigma_{xx}$ are both reduced by the presence of a perpendicular 12 T magnetic field. To quantify longitudinal conductivity in the presence of magnetic field, we measured both the electrical and the thermal Hall resistivities and inverted the resistivity tensor.

The field-induced decrease in electrical conductivity σ_{xx} (i.e., the magnetoresistance) was the subject matter of a previous study [44], which found that both longitudinal and transverse conductivity follow the behavior expected in the semiclassical picture:

$$\sigma_{xx} = \frac{ne\mu}{1 + \mu^2(\mu_0 H)^2}, \quad (2)$$

$$\sigma_{xy} = \frac{ne\mu}{1 + \mu^2(\mu_0 H)^2}\mu(\mu_0 H). \quad (3)$$

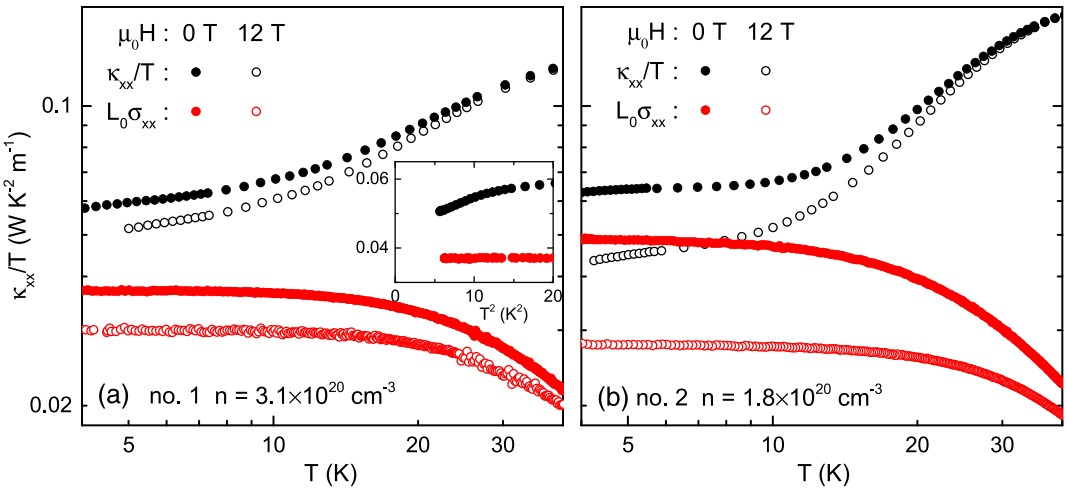

FIG. 1. Thermal conductivity in Nb-doped $SrTiO_3$. Thermal conductivity divided by temperature (κ_{xx}/T) at $\mu_0 H = 0$ and $\mu_0 H = 12$ T compared with the electrical conductivity multiplied by the Sommerfeld value ($L_0\sigma_{xx}$) in sample no. 1 (a) and in sample no. 2 (b). κ_{xx}/T increases with warming, because of the phonon contribution, which rises faster than T. $L_0\sigma_{xx}$, which is a rough estimate of electronic contribution to κ_{xx}/T decreases with warming due to the reduction of electrical conductivity by inelastic scattering. Note the reduction induced by magnetic field in both. The inset is an enlargement of the low-temperature data, showing that they tend to join in the zero-temperature limit.

Here, n is the carrier density and e is the electron charge. Mobility $\mu(T,\mu_0 H)$ is the only adjustable parameter depending on temperature and magnetic field. It monotonically decreases with increasing magnetic field and/or temperature. A remarkable (and poorly understood) fact about metallic STO is that the field dependence of mobility shows little dependence on the orientation of the magnetic field [44].

The thermal conductivity tensor $\bar{\kappa}$, on the other hand, has an electronic $\overline{\kappa^e}$ and a lattice $\overline{\kappa^{\rm ph}}$ component in longitudinal: $\kappa_{xx}(\mu_0 H) = \kappa^e_{xx}(\mu_0 H) + \kappa^{\rm ph}_{xx}$.

As in previous studies on semimetals [29,38,39], we separated the two components by assuming that the field dependence is negligibly small for the lattice component in comparison to the electronic component. In insulating strontium titanate, where thermal conductivity is purely phononic, a magnetic field of 12 T reduces the peak κ_{xx} at most by 7×10^{-3} [45] and generates a finite thermal Hall conductivity of $\kappa^{\rm ph}_{xy} \approx 0.09$ W/Km. In our metallic samples, the effect of magnetic field on κ^e_{xx} and the amplitude of κ^e_{xy} (see below) are orders of magnitude larger.

Figure 2 shows the temperature dependence of the transverse thermal conductivity divided by temperature $(-\kappa_{xy}/T)$. In the whole temperature range, it remains close (but smaller than $L_0\sigma_{xy}$), which is what is expected. The measured signal is much larger than $\kappa^{\rm ph}_{xy}/T$ measured in insulating STO [45,46].

Thus, we can safely identify the field-induced change in thermal conductivity $\Delta\kappa_{xx}$ with the thermal magnetoresistance of electrons:

$$\Delta\kappa_{xx} = \kappa^e_{xx}(\mu_0 H = 0) - \kappa^e_{xx}(\mu_0 H). \tag{4}$$

Figures 2(a) and 2(c) compare $\Delta\kappa_{xx}/T$ with $L_0\Delta\sigma_{xx}$. In both samples, these two quantities converge at low temperature and their difference grows with increasing temperature. This implies the validation of the WF law at zero temperature, a departure from it at finite temperature. The finite-temperature departure from the WF law is more significant in the sample with lower carrier density.

In order to extract the longitudinal electronic thermal conductivity at zero magnetic field $[\kappa^e_{xx}(\mu_0 H = 0)]$ from thermal magnetoconductivity $(\Delta\kappa_{xx})$, we need an additional assumption: At any given temperature, the field dependence of κ^e_{xx} is similar to the field dependence of the electrical conductivity [expressed by Eq. (2)]. Since the field-induced reduction in conductivity, in both thermal and electrical channels, is due to the same Lorentz force, this is reasonable. It implies that the Lorenz ratio $[L = (\kappa^e_{xx}/\sigma_{xx}T)]$ has a negligible field dependence, consistent with our field-dependent data (see Fig. S2 in the Supplemental Material [41]). Thus, magnetoresistance is set by the field dependence of residual resistivity and there is no detectable field-induced change in inelastic scattering.

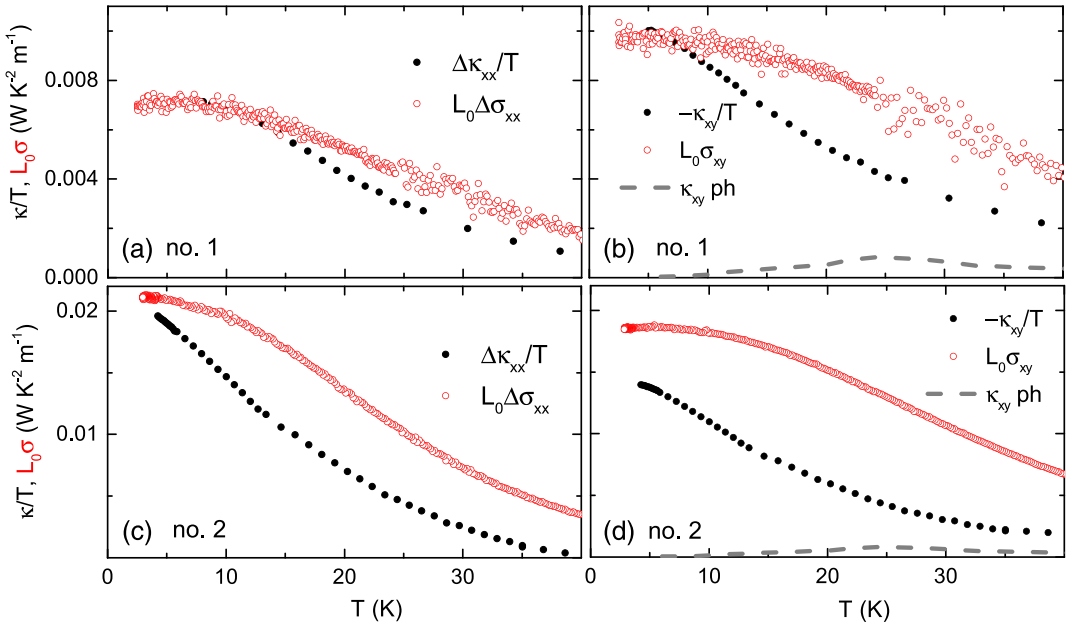

FIG. 2. Longitudinal and Hall conductivity. (a) The difference in longitudinal thermal conductivity divided by temperature between zero field and 12 T. $[\Delta\kappa_{xx} = \kappa_{xx}(0\ \mathrm{T}) - \kappa_{xx}(12\ \mathrm{T})]$ in sample no. 1. Also shown is the difference in the longitudinal electric conductivity multiplied by the Sommerfeld value $[\Delta\sigma_{xx} = \sigma_{xx}(0\ \mathrm{T}) - \sigma_{xx}(12\ \mathrm{T})]$. (c) Same for sample no. 2. (b) The transverse thermal conductivity κ_{xy} divided by temperature, compared with the transverse electric conductivity σ_{xy} multiplied by L_0. (d) Same for sample no. 2. Also shown in (b) and (d) is the κ_{xy}/T caused by phonons in undoped pure STO [37,45].

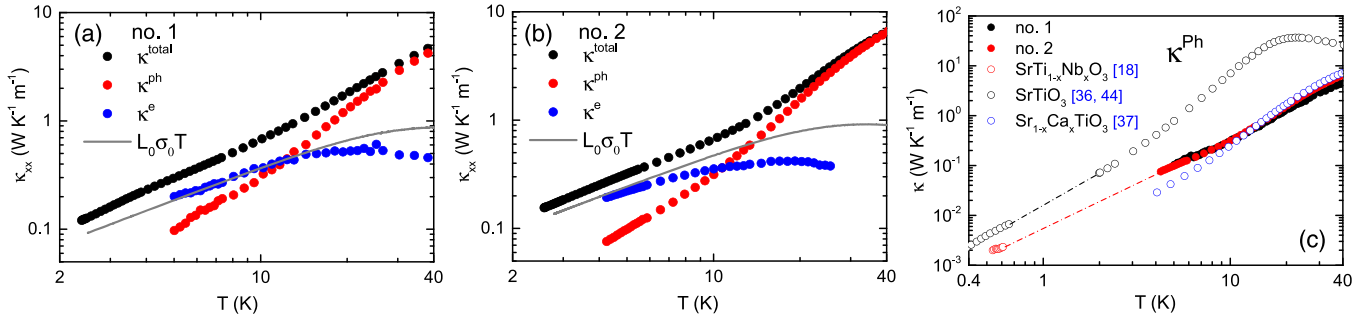

FIG. 3. Electron and phonon contributions to the thermal conductivity. (a) The total thermal conductivity ($\kappa_{xx}^{\text{total}}$) and its electronic ($\kappa_{xx}^{e}$) and phononic ($\kappa_{xx}^{\text{ph}}$) components as a function of temperature in sample no. 1. Also shown is the electrical conductivity multiplied by L_0. (b) Same for sample no. 2. (c) Comparison of the phonon thermal conductivity in the two samples with total thermal conductivity of undoped STO [36,47] with κ_{xx}^{ph} in $SrTi_{1-x}Nb_xO_3$, $n = 2.6 \times 10^{20}$ cm^{-3}, just above the superconducting transition [18] and with $Sr_{0.991}Ca_{0.009}TiO_3$ [37].

This approach leads us to [41]

$$\kappa_{xx}^{e}(\mu_0 H = 0) = \Delta\kappa_{xx}\frac{\sigma_{xx}(\mu_0 H = 0)}{\Delta\sigma_{xx}}. \tag{5}$$

Subtracting κ_{xx}^{e} from the total conductivity leads us to κ_{xx}^{ph}. Figure 3 shows the results. One can see that, above 20 K, κ_{xx}^{ph} becomes an order of magnitude larger than κ_e. However, since κ_{xx}^{ph} decreases faster than κ_{xx}^{e} with cooling, the electron contribution becomes prominent below 10 K. Almost equal to $L_0\sigma_0 T$ at low temperature, it significantly deviates downward at higher temperatures.

The extracted κ_{xx}^{ph}, shown in Fig. 3(c), is significantly lower than κ_{xx}^{ph} in undoped STO [36]. As one can see in the figure, κ^{ph} of our metallic samples, with about 1% of Ti atoms replaced by Nb, is similar to the total κ of insulating samples of $Sr_{1-x}Ca_xTiO_3$, with about 1% of Sr atoms replaced by Ca. In both cases, κ^{ph} is reduced in comparison to pristine STO, because the substituting atoms are randomly distributed and their average distance is comparable to the wavelength of thermally excited phonons. The rough similarity between Nb doping (which brings mobile electrons) and Ca substitution (which does not) indicates that scattering by mobile electrons plays a minor role.

Let us now turn our attention to WT, the inverse of κ_{xx}^{e}/T. Figure 4 shows ρ and L_0WT as a function of T^2. One can see that in both samples ρ_0 and L_0WT_0 are identical at low temperature, confirming the validity of the WF law in the zero-temperature limit. In both samples, the slope of $L_0WT(T^2)$ [that is, B] is larger than the slope of $\rho(T^2)$ [that is, A]. This behavior is similar to what has been observed in semimetals (like W, WP_2, and Sb) and heavy fermions (like UPt_3 and $CeRhIn_5$) (see Table S1 in the Supplemental Material [41]) and corresponds to what is theoretically expected in the e-e scattering picture [25].

The fermiology of doped strontium titanate is known [14,17,18,48,49]. Experiments have confirmed that, as expected by band calculations [14], three bands associated with Ti orbitals are successively filled, as the doping increases. In the two samples studied here, the carrier density is such that the Fermi surface consists of three concentric pockets, all three centered at the Γ point. The average radius of the outer pocket is bounded by the carrier

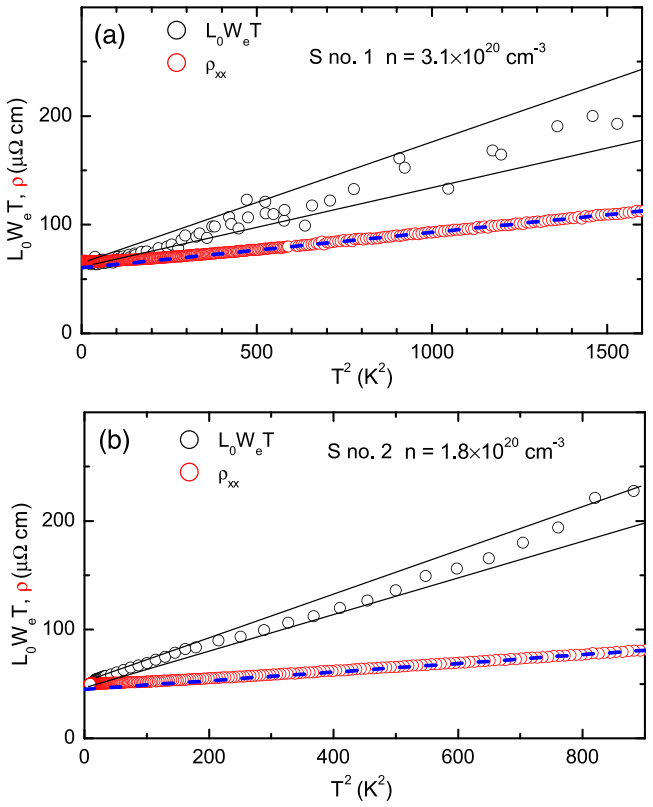

FIG. 4. Electronic thermal resistivity. (a) Electric and thermal resistivity as a function of the square of the temperature for sample no. 1. (b) Same as in (a) for sample no. 2. In both cases, ρ and WT have the same intercept but different slopes. The two black solid lines show the lower and the upper limit to the slope of thermal resistivity in the two samples.

TABLE I. Comparison with ^{3}He. Thermal conductivity, fermion-fermion scattering, and Fermi liquid properties in a strongly correlated and a weakly correlated fermionic system.

System	κT (W m)	v_F (m/s)	k_F (nm^{-1})	E_F (K)	$\tau_\kappa T^2$ (ns K^2)	ζ
^{3}He (saturating vapor pressure)	2.9×10^{-4}	60	7.9	1.8	3.9×10^{-4}	35
^{3}He (melting pressure)	7.3×10^{-5}	32.4	8.9	1.1	1.4×10^{-4}	58
$SrTi_{3-x}Nb_xO_3$ ($n = 3.1 \times 10^{20}$ cm^{-3})	27 ± 6	6×10^4	2.1	480	1.4	2.6 ± 0.6
$SrTi_{3-x}Nb_xO_3$ ($n = 1.8 \times 10^{20}$ cm^{-3})	13 ± 1.5	5×10^4	1.7	330	0.8	3.2 ± 0.3

density: $k_F^{\max} < (3\pi^2 n)^{1/3}$. This yields 2.1 (1.7) nm^{-1} in sample no. 1 (no. 2). The width of the Brillouin zone is $G = (2\pi/a) = 16.1$ nm^{-1}, where $a = 0.3905$ nm is the lattice parameter. Since $k_F^{\max} < (G/4)$, umklapp events cannot occur. This distinguishes metallic strontium titanate from other metals displaying T-square ρ and WT with linked amplitudes.

The other Fermi liquid with a T-square thermal resistivity in the absence of umklapp is normal liquid ^{3}He [50,51]. The dominant contribution to thermal conductivity (in the zero-temperature limit) is proportional to the inverse of temperature. This κT term is strictly equivalent to the inverse of B, the slope of WT as a function T^2, and, as first calculated by Abrikosov and Khalatnikov [52], is proportional to the fermion-fermion scattering time, which quadratically decreases with temperature. Extracted from thermal conductivity, this scattering time was dubbed τ_κ, and $\tau_\kappa T^2$ was extensively measured by Greywall [34]. Theoretically, this quantity was computed by quantifying the Landau parameters of the Fermi liquid [53–55]. The agreement between the theoretically computed and the experimentally measured κT and $\tau_\kappa T^2$ is within experimental uncertainty at saturating vapor pressure and less than a factor of 2 near the melting pressure.

Let us now see how metallic strontium titanate fits in this picture. τ_κ is given by [34]

$$\kappa = \frac{1}{3}\frac{C_V}{V_m} v_F^2 \tau_\kappa. \tag{6}$$

Here, C_V is the molar specific heat, V_m is the molar volume, and v_F the Fermi velocity. This means that, in analogy with the case of normal liquid ^{3}He [34], B, the prefactor of T-square thermal resistivity, is inversely proportional to $\tau_\kappa T^2$:

$$\frac{1}{\tau_\kappa T^2} = \frac{v_F^2}{3}\frac{\gamma}{V_m} B. \tag{7}$$

Using the reported values of γ (ranging from 1.55 to 1.9 mJ/mol K^2 [19,35,56] at this doping level) and extracting the average Fermi wave vector from carrier density, one can quantify the Fermi velocity and find $\tau_\kappa T^2$. The results are listed in Table I. Unsurprisingly, $\tau_\kappa T^2$ is orders of magnitude larger in STO than in ^{3}He, which has a lower Fermi temperature and higher fermion-fermion collision cross section.

A more instructive basis for comparison is a dimensionless collision cross section defined as [55,57–59]

$$\zeta = \frac{\hbar E_F}{\tau_\kappa T^2 k_B^2}. \tag{8}$$

The amplitude of this quantity in a Fermi liquid is set by a combination of its Landau parameters [57,60,61]. As seen in Table I, ζ in ^{3}He, strongly correlated and close to both localization and a magnetic instability [62], varies from 35 to 60. In contrast, ζ in STO, at this doping level (where the effective mass is close to 4 times the bare electron mass [16,35]), is $\approx$3.

Thus, not only the existence of the T-square thermal resistivity in metallic strontium titanate but also its amplitude can be accounted for by considering it as a Fermi liquid with moderate correlations. As for T-square electrical resistivity (at low temperatures, that is below the degeneracy temperature of electrons and the minimum energy of the soft TO phonons), it could be accounted for, assuming a rough recovery of the Wiedemann-Franz law in the presence of disorder. However, the theory for such a scenario is yet to be elaborated. It may require including the gradient of momentum flow caused by disorder and phonon scattering.

We thank L. Hechler, M. Feigel'man, X. Li, A. Marguerite, D. Maslov, D. Vollhardt P. Wölfle, and Z. Zhu for discussions. This work was supported by the Agence Nationale de la Recherche (ANR-19-CE30-0014-04), by Jeunes Equipes de l'Institut de Physique du Collège de France, and by a grant by the Ile de France Regional Council. S. J. acknowledges a grant from China Scholarship Council.

[1] L. Landau and I. Pomeranchuk, Phys. Z. Sowjetunion **10**, 649 (1936).
[2] W. Baber, Proc. R. Soc. A **158**, 383 (1937).
[3] R. Joynt and L. Taillefer, Rev. Mod. Phys. **74**, 235 (2002).
[4] Y. Maeno, K. Yoshida, H. Hashimoto, S. Nishizaki, S.-i. Ikeda, M. Nohara, T. Fujita, A. Mackenzie, N. Hussey, J. Bednorz, and F. Lichtenberg, J. Phys. Soc. Jpn. **66**, 1405 (1997).

[5] R. Hartman, Phys. Rev. **181**, 1070 (1969).
[6] C. Uher and W. P. Pratt, Phys. Rev. Lett. **39**, 491 (1977).
[7] K. Yamada and K. Yosida, Prog. Theor. Phys. **76**, 621 (1986).
[8] H. Maebashi and H. Fukuyama, J. Phys. Soc. Jpn. **67**, 242 (1998).
[9] M. Rice, Phys. Rev. Lett. **20**, 1439 (1968).
[10] K. Kadowaki and S. Woods, Solid State Commun. **58**, 507 (1986).
[11] N. Tsujii, K. Yoshimura, and K. Kosuge, J. Phys. Condens. Matter **15**, 1993 (2003).
[12] N. E. Hussey, J. Phys. Soc. Jpn. **74**, 1107 (2005).
[13] T. Okuda, K. Nakanishi, S. Miyasaka, and Y. Tokura, Phys. Rev. B **63**, 113104 (2001).
[14] D. van der Marel, J. L. M. van Mechelen, and I. I. Mazin, Phys. Rev. B **84**, 205111 (2011).
[15] X. Lin, B. Fauqué, and K. Behnia, Science **349**, 945 (2015).
[16] C. Collignon, X. Lin, C. W. Rischau, B. Fauqué, and K. Behnia, Annu. Rev. Condens. Matter Phys. **10**, 25 (2019).
[17] X. Lin, Z. Zhu, B. Fauqué, and K. Behnia, Phys. Rev. X **3**, 021002 (2013).
[18] X. Lin, A. Gourgout, G. Bridoux, F. Jomard, A. Pourret, B. Fauqué, D. Aoki, and K. Behnia, Phys. Rev. B **90**, 140508 (R) (2014).
[19] E. McCalla, M. N. Gastiasoro, G. Cassuto, R. M. Fernandes, and C. Leighton, Phys. Rev. Mater. **3**, 022001(R) (2019).
[20] C. Collignon, P. Bourges, B. Fauqué, and K. Behnia, Phys. Rev. X **10**, 031025 (2020).
[21] A. Kumar, V. I. Yudson, and D. L. Maslov, Phys. Rev. Lett. **126**, 076601 (2021).
[22] K. G. Nazaryan and M. V. Feigel'man, Phys. Rev. B **104**, 115201 (2021).
[23] J. Wang, J. Wu, T. Wang, Z. Xu, J. Wu, W. Hu, Z. Ren, S. Liu, K. Behnia, and X. Lin, Nat. Commun. **11**, 3846 (2020).
[24] J. Ziman, *Principles of the Theory of Solids* (Cambridge University Press, Cambridge, England, 1972).
[25] S. Li and D. L. Maslov, Phys. Rev. B **98**, 245134 (2018).
[26] G. White and R. Tainsh, Phys. Rev. Lett. **19**, 165 (1967).
[27] J. Garland and D. Van Harlingen, J. Phys. F **8**, 117 (1978).
[28] D. Wagner, J. Garland, and R. Bowers, Phys. Rev. B **3**, 3141 (1971).
[29] A. Jaoui, B. Fauqué, and K. Behnia, Nat. Commun. **12**, 195 (2021).
[30] J. Paglione, M. A. Tanatar, D. G. Hawthorn, R. W. Hill, F. Ronning, M. Sutherland, L. Taillefer, C. Petrovic, and P. C. Canfield, Phys. Rev. Lett. **94**, 216602 (2005).
[31] A. Jaoui, B. Fauqué, C. W. Rischau, A. Subedi, C. Fu, J. Gooth, N. Kumar, V. Süß, D. L. Maslov, C. Felser *et al.*, npj Quantum Mater. **3**, 64 (2018).
[32] B. Lussier, B. Ellman, and L. Taillefer, Phys. Rev. Lett. **73**, 3294 (1994).
[33] K. Behnia, Ann. Phys. (Berlin) **534**, 2100588 (2022).
[34] D. S. Greywall, Phys. Rev. B **29**, 4933 (1984).
[35] X. Lin, G. Bridoux, A. Gourgout, G. Seyfarth, S. Krämer, M. Nardone, B. Fauqué, and K. Behnia, Phys. Rev. Lett. **112**, 207002 (2014).
[36] V. Martelli, J. L. Jiménez, M. Continentino, E. Baggio-Saitovitch, and K. Behnia, Phys. Rev. Lett. **120**, 125901 (2018).
[37] S. Jiang, X. Li, B. Fauqué, and K. Behnia, Proc. Natl. Acad. Sci. U.S.A. **119**, e2201975119 (2022).
[38] G. K. White and S. B. Woods, Philos. Mag. A **3**, 342 (1958).
[39] C. Uher and H. J. Goldsmid, Phys. Status Solidi (b) **65**, 765 (1974).
[40] A. Jaoui, A. Gourgout, G. Seyfarth, A. Subedi, T. Lorenz, B. Fauqué, and K. Behnia, Phys. Rev. X **12**, 031023 (2021).
[41] See Supplemental Material at http://link.aps.org/supplemental/10.1103/PhysRevLett.131.016301 for additional data regarding the samples and the experimental techniques as well as a discussion of methodology, which includes Refs. [13,20,28–32,37,42,43].
[42] J. Paglione, M. A. Tanatar, D. G. Hawthorn, F. Ronning, R. W. Hill, M. Sutherland, L. Taillefer, and C. Petrovic, Phys. Rev. Lett. **97**, 106606 (2006).
[43] A. Spinelli, M. A. Torija, C. Liu, C. Jan, and C. Leighton, Phys. Rev. B **81**, 155110 (2010).
[44] C. Collignon, Y. Awashima, Ravi, X. Lin, C. W. Rischau, A. Acheche, B. Vignolle, C. Proust, Y. Fuseya, K. Behnia, and B. Fauqué, Phys. Rev. Mater. **5**, 065002 (2021).
[45] X. Li, B. Fauqué, Z. Zhu, and K. Behnia, Phys. Rev. Lett. **124**, 105901 (2020).
[46] In STO samples with a carrier density 2 orders of magnitude lower ($n \approx 10^{18}$ cm^{-3}), κ_{xy}/T is larger than $L_0\sigma_{xy}$, in contrast with the samples studied here, where the Hall angle is much smaller than unity and one does not expect a detectable phonon drag contribution to κ_{xy} (see Supplemental Material [41]).
[47] C. W. Rischau, Y. Li, B. Fauqué, H. Inoue, M. Kim, C. Bell, H. Y. Hwang, A. Kapitulnik, and K. Behnia, Phys. Rev. Lett. **126**, 077001 (2021).
[48] S. J. Allen, B. Jalan, S. B. Lee, D. G. Ouellette, G. Khalsa, J. Jaroszynski, S. Stemmer, and A. H. MacDonald, Phys. Rev. B **88**, 045114 (2013).
[49] B. Fauqué, C. Collignon, H. Yoon, Ravi, X. Lin, I. Mazin, H. Y. Hwang, and K. Behnia, arXiv:2208.09831.
[50] E. R. Dobbs, *Helium Three* (Oxford University Press, New York, 2000).
[51] A. J. Leggett, Rep. Prog. Phys. **79**, 054501 (2016).
[52] A. A. Abrikosov and I. M. Khalatnikov, Rep. Prog. Phys. **22**, 329 (1959).
[53] K. S. Dy and C. J. Pethick, Phys. Rev. **185**, 373 (1969).
[54] J. Sykes and G. A. Brooker, Ann. Phys. (N.Y.) **56**, 1 (1970).
[55] P. Wolfle, Rep. Prog. Phys. **42**, 269 (1979).
[56] E. Ambler, J. H. Colwell, W. R. Hosler, and J. F. Schooley, Phys. Rev. **148**, 280 (1966).
[57] M. Pfitzner, J. Low Temp. Phys. **61**, 141 (1985).
[58] D. Vollhardt and P. Wolfle, *The Superfluid Phases of Helium 3* (CRC Press, Boca Raton, FL, 1990).
[59] K. Behnia, SciPost Phys. **12**, 200 (2022).
[60] M. Pfitzner and P. Wölfle, J. Low Temp. Phys. **51**, 535 (1983).
[61] M. Pfitzner and P. Wölfle, Phys. Rev. B **35**, 4699 (1987).
[62] D. Vollhardt, Rev. Mod. Phys. **56**, 99 (1984).